ARTICLE

Exploring structure based charge transport relationships in phenyl diketopyrrolopyrrole single crystals using a 2D π-π dimer model system

Jesus Calvo-Castro[a] and Callum J. McHugh[b]

Crystalline phenyl diketopyrrolopyrroles are often overlooked as charge transfer mediating materials in optoelectronic applications. We report an experimentally ratified two dimensional π-π model dimer system dispelling previous misconceptions regarding the potential of these materials as organic semiconductors and that will enable researchers to screen and predict charge transport potential solely on the basis of their single crystal derived π-stacking architectures. In testing our model system versus the available database of phenyl diketopyrrolopyrrole single crystal structures we reveal that these materials are characterised by intrinsically large thermal integrities and in many cases large charge transfer integrals, not solely restricted to dimeric interactions exhibiting close intermonomer arrangements and bearing low torsion of the core phenyl rings. This study will be of significant interest to the increasingly large community engaged in the quest to engineer π-conjugated organic based semiconducting devices and particularly those employing crystalline diketopyrrolopyrroles.

Introduction

Achieving optimal charge carrier mobility in small molecule π-conjugated organic semiconducting devices, where π-π interactions facilitate charge mobility and one and two-dimensional π-stacking motifs provide desirable charge propagation channels for effective charge transfer phenomenon, is at the forefront of current research interests and efforts.[1-3] It is widely acknowledged that organic single crystals (OSCs) are critical in realising effective performance in optoelectronic devices bearing organic conjugated architectures, given their superior purity and longer range structural order in relation to crystalline or amorphous thin films.[1, 3-5] Despite these advantages, most reported mobility measurements in the literature are based on crystalline and amorphous thin film architectures where mobility values can be negatively influenced through the presence of grain boundaries and defects. Thus, in some cases, potentially good charge mediators can be overlooked solely on the basis of poor preliminary results that may be a consequence of device manufacturing and not intrinsic molecular properties.[2]

In this regard, significant efforts have been devoted to develop an in-depth understanding of the role that systematic substitutions on common core motifs can exert on charge carrier properties and

subsequent device performance.[2, 6-11] *In-silico* design based upon an evaluation of intrinsic material properties which dictate charge transport behavior and subsequent performance in organic semiconductors represents a highly prized asset in materials development, providing a tool that can facilitate the identification of superior materials by molecular argument. Among the numerous types of small π-conjugated systems investigated, diketopyrrolopyrrole (DPP) based materials, largely employed in industry as high performance pigments,[12, 13] have more recently attracted an increasing surge of interest in optoelectronics.[13-15] Most reported experimental studies of DPPs, including both polymers and small molecules, utilize thiophene core rings instead of phenyl substituents. This contrasts with the significantly larger number of phenyl (77) vs thiophene (28) DPP single crystal structures contained in the Cambridge Structural Database (CSD). Contrary to a popular notion that phenyl-substituted DPPs (**PDPP**s) are not structurally optimal for OFET applications,[15] we have recently demonstrated that phenyl-based DPP architectures represent a theoretically superior alternative to equivalent thiophene and furan-based systems,[16] particularly in crystalline hole transport environments. Via judicious choice of aryl and N-substituents, **PDPP** single crystal structures can exhibit comparable or even greater charge transfer integrals than rubrene, for which mobilities of 20 cm^2 V^{-1} s^{-1} have been reported in the crystalline state.[17]

Inspired by this outcome, in the following we report a comprehensive analysis of intermolecular interactions and associated charge transfer integrals for a dimeric **PDPP** model system by simultaneously modifying the long and short molecular axes shifts which govern π-π stacking interactions and wavefunction overlap. We investigate the effect of core phenyl ring torsion on

---
[a.] *School of Life and Medical Sciences, University of Hertfordshire, Hatfield, AL10 9AB, UK.*
[b.] *School of Science and Sport, University of the West of Scotland, Paisley, PA1 2BE, UK.*

these properties and ultimately challenge and validate our proposed two-dimensional model system by screening all phenyl-based DPP crystal structures reported to date. Impressively, experimentally observed device mobility data are clearly accounted for based on the model dimer predictions. It should be noted that although other crystal extracted dimer pairs can exhibit large binding energies, such as those with strong H-bonding intermolecular interactions, they do not represent optimal charge transfer propagation channels, on account of their diminished electronic coupling.[8-11, 16]
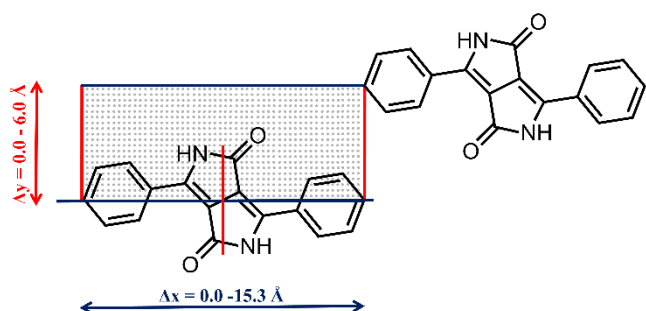

Figure 1. Illustration of long (blue) and short (red) intermonomer displacements in our **PDPP** dimer model system. Grey filled circles illustrate x/y locations of single point calculations.

The reported dimer system was constructed with single point calculations employing Truhlar's density functional M06-2X,[18] which has been shown to give a good account of intermolecular interactions dominated by non-covalent interactions,[8, 9, 19] and the triple-zeta basis set, 6-311G(d), previously reported to perform well with regards to charge penetration effects at interplanar distances lower than 4 Å,[8] as implemented in Spartan 10 software.[20] For a number of key dimer pairs, calculations were corroborated using the ωB97X-D[21] density functional. An increase (32% on average) in interaction energy and little difference in the computed charge transfer integrals were observed (ESI). Dimer interactions were all corrected for basis set superposition error using the counterpoise corrected method[22] and charge transfer integrals were computed within the framework of the energy-splitting-in-dimer method for symmetric systems,[23] with all dimer pairs investigated in this work being centrosymmetric. The two phenyl-substituted DPP monomers were mutually aligned in a fully eclipsed arrangement, separated by an optimum interplanar distance of 3.6 Å.[8, 9] Whilst fixing the coordinates of the bottom monomer, the top monomer was displaced along the long (x) and short (y) molecular axes simultaneously[9, 19, 23-25] in increments of 0.3 Å over a distance of 15.3 and 6.0 Å respectively. This generated a two-dimensional surface bearing 12 single point calculations per Å^2, covering the broad diversity of intermonomer shifts observed in π-π dimer pairs of **PDPP** crystal structures reported to date (Table 1).

Results and discussion

Two-dimensional π-π dimer model

Computed counterpoise corrected intermolecular interactions for the **PDPP** dimer model system as a function of long and short molecular axes displacements are illustrated in Figure 2. The position of the local minima throughout the potential energy surface can be ascribed to favourable local bond dipole/bond dipole and induced bond dipole interactions, which dictate strong slipped cofacial intermolecular interactions at ca. Δx = 1.5, 3.3, 5.4, 7.5 and 10.2 Å.[8, 9] Through analysis of the CSD output, it is apparent that specific substitution of the **PDPP** motif can also lead to systematic shifts along the short molecular axis.[10, 11] From analysis of the computed intermolecular interactions illustrated in Figure 2, we observe that particularly strong binding interactions are not solely restricted to geometries exhibiting Δy = 0.0 but can also be found in dimer pairs characterised by $\Delta y \leq 2.1$ Å. The global minimum (ΔE_{CP} = -54.69 kJ mol^{-1}) of the model was found at Δx and Δy of 3.3 and 0.3 Å respectively, where the C-C linker between core and phenyl rings of one monomer is superposed with respect to the DPP core of the other and vice-versa (Figure 2). Analogous strong ΔE_{CP} were observed at $\Delta x/\Delta y$ of 3.9/0.6 (ΔE_{CP} = -53.38 kJ mol^{-1}) and 3.6/0.9 Å (ΔE_{CP} = -50.51 kJ mol^{-1}) respectively. Given the large sensitivity of charge transfer properties to small changes in intermolecular shifts (*vide infra*), it is of particular interest that dimer pairs characterised by large displacements along the short molecular axis exhibit greater binding energies (ΔE_{CP} = -38.28 kJ mol^{-1} for $\Delta x/\Delta y$ = 5.7/2.1 Å respectively) than that of rubrene (ΔE_{CP} = -35.60 kJ mol^{-1}). This illustrates the inherently greater thermal integrity of **PDPP** architectures, which is a very desirable property in charge transfer mediating materials, where thermally induced motion and distortion of the crystal lattice can have a detrimental impact on
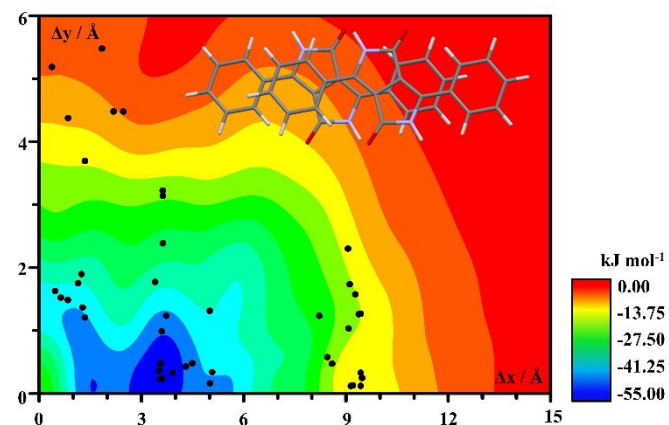
charge transfer integrals and bandwidth.[26]

Figure 2. Two-dimensional map illustrating computed intermolecular interactions of **PDPP** dimer model system. Inset represents **PDPP** dimer pair geometry at the global minimum. Black filled circles denote $\Delta x/\Delta y$ positions of reported PDPP-based dimer pairs.

Inspection of the computed hole and electron charge transfer integrals illustrated in Figure 3, which are consistent with nodal progression of the monomer frontier molecular orbitals along both monomer axes, reveals particularly large values at long molecular axis shifts, Δx, of ca 0.7/2.5/5.0/7.5 and 0.6/2.0/4.0/6.2/8.0 Å for t_h and t_e respectively. Electronic coupling propagates along the short molecular axis to a greater extent in t_e (ca Δy = 3.0 Å) than in t_h (ca

Δx = 2.0 Å). Thus, large hole and electron mobilities in **PDPP**-based systems are not solely restricted to dimer pairs characterised by close long molecular axis alignment. Of interest to us was the complete reversal of the charge transfer properties afforded by small shifts along both molecular axes, particularly striking on progression from dimer pairs exhibiting Δx/Δy of 3.9/0.3 and 5.4/0.3 Å, with computed t_h/t_e of 1.65/13.74 and 10.26/1.26 kJ mol^{-1} respectively and an energy barrier of 7.27 kJ mol^{-1}. We anticipate that **PDPP**-based architectures may offer a clear potential for the realization of thermally activated reversal of the charge transfer character.

PDPP systems are often undervalued as organic semiconductors on account of reduced planarity when compared to thiophene and furan analogues,[16] despite their comparable computed inner-sphere reorganization energies at torsional angles often observed in crystalline environments. It was therefore of interest to explore the effects of planarity on the intermolecular interactions and charge transfer integrals for fully eclipsed (Δx/Δy of 0.0/0.0 Å) and two-dimensional model global minimum (Δx/Δy of 3.3/0.3 Å) dimer pairs by systematically increasing the dihedral angle of the core phenyl rings with respect to the DPP core. Whilst core phenyl ring torsions can lead to differences in crystalline packing arrangements,[9] we observe that contrary to popular belief,[15] the increased torsion of the phenyl rings with respect to the planar DPP core from θ = 0 to 50 °, affords a slight enhancement of the electron and hole transfer properties in the two dimer pairs studied. In short, for the fully eclipsed dimer pair, t_h/t_e vary from 26.20/28.94 to 27.85/30.54 kJ mol^{-1} for θ = 0 and 50° respectively, consistent with an increased overlap and associated bonding/anti-bonding character of the supramolecular orbitals. Similarly, for the global minimum dimer geometry, t_h/t_e vary from 7.77/5.03 to 9.83/5.02 kJ mol^{-1} for θ = 0 and 50 ° respectively, going through a maximum transfer integral at θ = 35 (t_h = 11.47 kJ mol^{-1}) and 25 ° (t_e = 9.00 kJ mol^{-1}) for t_h and t_e respectively.
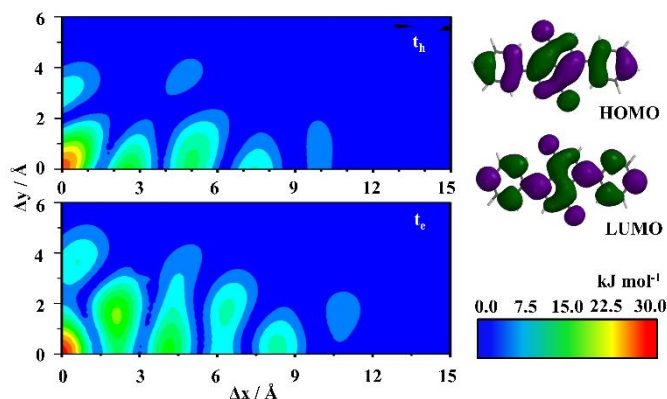

Figure 3. Two-dimensional map illustrating computed hole, t_h (top) and electron, t_e (bottom) transfer integrals of **PDPP** dimer model system and frontier molecular orbital surfaces of **PDPP** monomer.

Intermolecular interactions and associated charge transfer integrals for reported PDPP based architectures

In the remainder of the paper we explore the theoretical charge transfer properties for every reported single crystal **PDPP** based structure in the CSD displaying one-dimensional π-π stacking behavior (37 out of the 77 deposited structures, Table 1).[6, 7, 9-11, 16,]

[27-45] Large ΔE$_{CP}$, indicating desirable thermal integrity was computed for every **PDPP** based architecture, with substitution of the lactam nitrogen and core phenyl rings contributing to and dictating the degree of intermonomer slip. We illustrate in Figure 2 that independently of short molecular axis shifts, values of Δx were consistent with areas of energy minima along the long molecular axis, with a particular higher density of structures occupying the broad energy minimum coordinates at Δx = 3 − 5 and Δy = 0 − 1 Å respectively. In addition, greater Δy were observed for pigmented analogues, which we attribute to packing arrangements largely determined by H-bonding interactions in the absence of N-substitution. Interestingly, we observed that large Δy are also exhibited by the particular N-substitution in **EBIGUR04** (Δy = 5.26 Å) and **XATKIN** (Δy = 3.80 Å) via N-boc and N-alkyl chains (C4) arranged perpendicularly to the DPP core plane, hence precluding close intermonomer arrangement along their short molecular axes (ESI).

Table 1. CSD identifier, measured intermonomer displacements, intermolecular interactions, ΔE$_{CP}$ (kJ mol^{-1}) and charge transfer integrals, t_h/t_e (kJ mol^{-1}) for π-π dimer pairs of reported **PDPP** crystal structures. *M062X/6-31G(d)

CSD identifier	Δ(xyz) / Å	ΔE$_{CP}$	t_h/t_e
EBIGUR04[27]	0.59/5.26/3.14	-58.90	1.10/2.86
EKUFAT[28]	1.34/1.18/3.92	-74.42	5.01/5.19
EKUFEX[28]	4.14/0.41/3.88	-52.25	2.69/3.71
EREHAM[11]	9.13/1.64/3.35	-41.08	0.27/0.79
	0.58/4.43/2.78	-56.17	3.47/5.12
FOVYAS[29]	3.40/1.01/3.31	-62.24	5.23/7.11
GATJIX[8]	3.57/0.23/3.42	-79.16	1.96/7.50
GAJTOD[8]	3.55/0.05/3.66	-79.36	2.17/4.54
GEGHUX[30]	9.42/0.15/3.71	-77.80	8.60/4.58
GEGJAF[30]	9.17/0.15/3.78	-100.16*	11.52/2.13*
GEGJEJ[30]	9.14/0.17/3.72	-140.89*	6.86/1.80*
GORLOQ[7]	3.45/0.30/3.37	-155.81	0.80/9.63
HEJCEG[31]	9.07/1.20/3.34	-96.55	3.97/4.11
HEJCOQ[31]	9.13/1.66/3.54	-61.19	0.12/0.73
HOZNER[9]	8.44/0.05/3.37	-39.46	1.02/5.09
HUTLEO[32]	8.44/0.47/3.78	-51.52	3.60/3.02
HUYZUW[33]	5.03/1.26/5.02	-51.09	1.71/0.08
KAWMUR[34]	1.06/1.90/5.33	-36.39	0.57/0.05
KAWNAY[34]	3.34/2.32/4.06	-66.67	5.07/6.93
LAHCIJ[35]	3.48/0.51/3.45	-103.45	5.54/15.11
MUNHEK[6]	3.46/3.09/3.26	-47.84	2.49/4.01
	2.37/4.35/3.15	-37.06	11.62/2.93
OKUZUQ[36]	8.26/1.21/3.66	-42.48	4.35/9.26
PAMYUY[37]	5.01/0.10/3.34	-68.82	14.58/4.82
QOHGAX[9]	4,52/0.05/3.44	-70.12	10.69/6.13
QOHGEB[9]	9.40/0.31/3.32	-35.52	6.03/1.41
QUYHIC[38]	3.28/1.80/4.10	-60.73	1.87/1.79
SAPDES[39]	1.82/5.52/2.92	-14.48	2.41/1.20
	0.68/1.51/3.27	-57.15	4.64/4.51
UKATOR[10]	3.72/0.35/3.90	-71.02	0.50/3.68
UKATUX[10]	9.12/2.31/3.59	-22.46	2.01/0.89
VARKII01[40]	1.28/1.47/4.08	-63.06	5.03/4.48
WEBKAP[41]	1.03/1.80/3.34	-67.45	9.48/1.87

WEBKET[41]	3.40/3.13/3.32	-48.11	1.75/2.27
	2.25/4.58/3.23	-36.13	9.51/3.11
WEPCUQ[42]	0.44/1.66/3.53	-43.39	2.72/4.97
WOHDAY[43]	0.91/1.53/3.36	-54.83	8.34/2.47
WUTCEU[44]	9.39/1.22/3.22	-42.51	4.38/1.67
WUTCEU01[9]	5.13/0.28/3.38	-69.60	11.77/3.96
WUTCEU02[9]	9.39/1.22/3.22	-42.51	4.38/1.67
XATKIN[45]	1.37/3.68/3.16	-58.64	0.44/3.80

Whilst intermolecular interactions are largely dictated by substitution of the lactam nitrogen atoms as well as the core phenyl rings, we note that underpinned by our previous work,[9-11] charge transfer integrals are not significantly influenced by N-substitution. This is readily understood by examination of the nodal progressions of the frontier molecular orbitals illustrated in Figure 3 and subsequent extension of conjugation through the lactam nitrogen atoms upon N-substitution. We report hole/electron transfer integrals that are greater or at least comparable to those computed by us for rubrene ($t_{h/e}$ = 12.39/7.50 kJ mol^{-1}) for 5/6 of the **PDPP** systems (Table 1), thus illustrating the potential of these materials as crystalline hole and electron transport materials.
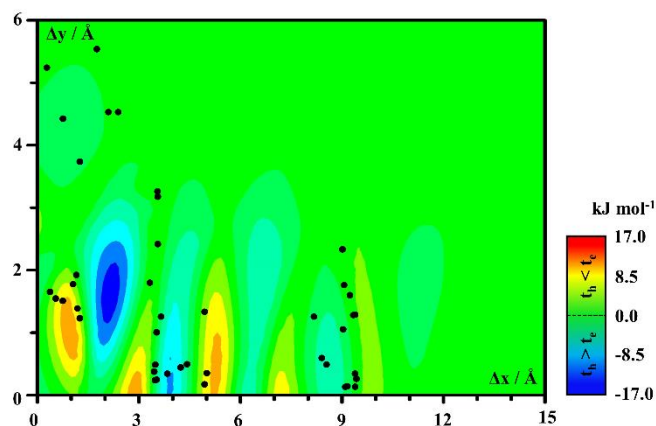

Figure 4. Two-dimensional map illustrating the dominance of t_h vs t_e and vice-versa. Black filled circles denote $\Delta x/\Delta y$ positions of reported **PDPP**-based π-π dimer pairs.

In addition, we compare the computed charge transfer integrals to those estimated using the proposed two-dimensional dimer model system and measured intermonomer displacement for each reported **PDPP**-based architecture (Table 1). In all cases but four, we observed a successful qualitative agreement between crystal derived dimer pairs and associated model dimer pairs in predicting the relative order of $t_h > t_e / t_h < t_e$, despite differences in the interplanar distance and phenyl ring torsional angles. The 'outlier' behavior of **GEGJAF, GEGJEJ, HUTLEO** and **WEPCUQ** can be accounted for on the basis of the thiophene, cyano and morpholine substitutions (ESI) along their long molecular axes respectively, and the associated impact on the nodal progression. Finally, experimental mobilities have been reported for three reported pigment architectures, **SAPDES**, **WEBKET** and **MUNHEK** which display H, Cl and Br substitution on the para position of the core phenyl rings respectively. These pigmented systems exhibit two distinct π-π dimer pairs (ESI), with the binding energy of one dimer pair outweighing that computed for its counterpart in all cases.

Given the role of large intermolecular interactions in preserving the thermal integrity of one-dimensional π-stacking charge propagation channels, we focus on the dimer pairs exhibiting greater ΔE_{CP}. Ambipolar character exhibited by the H substituted analogue ($\mu_{h/e}$ = 0.01 cm^2 V^{-1} s^{-1}), **SAPDES**, is well accounted for by our calculations on crystal structure geometries (t_h/t_e = 4.64/4.51 kJ mol^{-1}) and associated model system (t_h/t_e = 0.67/0.51 kJ mol^{-1}), with differences in absolute charge transfer integrals ascribed to changes in intermonomer distance along the z axis (Δz = 3.60 and 3.27 Å for crystal derived and model dimer pairs respectively). Higher electron than hole mobilities in chlorinated and brominated architectures ($\mu_{h/e}$ = 0.01/0.03 and 0.02/0.06 cm^2 V^{-1} s^{-1} for Cl and Br substituted systems respectively) are also in agreement with our calculations in crystal derived dimers ($t_{h/e}$ = 1.75/2.27 and 2.49/4.01 kJ mol^{-1} for Cl- and Br-**PDPP** respectively). The larger values for Br containing systems are readily ascribed to its greater polarizability.[8, 9] Hole mobilities were also reported for another two series of **PDPP** architectures. In the case of **GEGHUX**, **GEGJAF** and **GEGJEJ**,[30] bearing one, two and three conjugated thiophene rings on the para position of the core phenyl rings respectively, greater hole mobilities were experimentally measured for **GEGJAF** (7.8 x 10^{-6} cm^2 V^{-1} s^{-1}) than for its structural analogues **GEGHUX** and **GEGJEJ** (4.6 x 10^{-6} and 2.4 x 10^{-6} cm^2 V^{-1} s^{-1} respectively), as theoretically determined for their single crystal extracted dimer pairs (t_h = 11.52, 8.60 and 6.86 kJ mol^{-1} for **GEGJAF**, **GEGHUX** and **GEGJEJ** respectively). Lastly, greater hole mobility was experimentally measured for the monosubstituted structure, **FOVYAS** than for its disubstituted analogue, **QUYHIC** (1.6 x 10^{-2} and 2.0 x 10^{-4} cm^2 V^{-1} s^{-1} respectively). This is in agreement with our theoretical calculations (t_h = 5.23 and 1.87 kJ mol^{-1} for **FOVYAS** and **QUYHIC** respectively) and associated with the greater displacement of the di-substituted analogue along the short molecular axis resulting in lowering the wavefunction overlap (ESI).

Table 2. Experimentally determined mobilities and computed charge transfer integrals for investigated systems.

CSD identifier	$t_{h/e}$ / kJ mol^{-1}	$\mu_{h/e}$ / cm^2 V^{-1} s^{-1}
SAPDES	4.64/4.51	0.01/0.01
WEBKET	1.75/2.27	0.01/0.03
MUNHEK	2.49/4.01	0.02/0.06
GEGHUX	8.60/4.58	4.60 x 10^{-6}/-
GEGJAF	11.52/2.13	7.80 x 10^{-6}/-
GEGJEJ	6.86/1.80	2.40 x 10^{-6}/-
FOVYAS	5.23/7.11	1.60 x 10^{-2}/-
QUYHIC	1.87/1.79	2.00 x 10^{-4}/-

Conclusions

In conclusion, we report an experimentally validated theoretical two dimensional π-π dimer model system for phenyl diketopyrrolopyrroles that dispels previous misconceptions regarding the potential application of these materials in organic optoelectronics and that will enable researchers to theoretically predict and therefore screen the charge transfer properties of any **PDPP** through simple analysis of single crystal derived dimer pair geometries. Our analysis reveals 11 existing **PDPP**s in the CSD that

exhibit hole and electron charge transfer integrals that are higher than those computed for the π-π stacks in rubrene. We recommend that single crystal devices from these materials should be fabricated and characterised with immediate effect. In fully accounting for all available database structures, we observe that π-π dimer pairs of **PDPP**s are characterised by large binding energies and high intrinsic thermal integrity. Our results imply that crystalline **PDPP**s may be interesting motifs from which to study the effects of dynamic disorder on charge transport. In addition, we predict that strong electronic coupling is not solely restricted to dimer pairs characterised by close intermonomer alignment in these single crystals or negatively influenced by phenyl torsional twists, thus extending the possible diversity in orientations that may be exploited to maximise optimal electronic behaviour. Our model system successfully predicts $t_h>t_e/t_h<t_e$ for 37 out of 41 crystal extracted π-π dimer pairs reported in the CSD despite a rich diversity of both core aryl and N-substituents in all of these structures, with the four outliers accounted for on the basis of substitution effects on the nodal progression through their long molecular axes displacements. Thus, we anticipate a broad applicability of our model, regardless of the N-substitution pattern employed. Experimentally determined mobilities reported for **PDPP** based architectures reported in the CSD are all well accounted for using our model, with the relative ordering of the measured and computed mobilities ratified on the basis of intermonomer displacements resulting from specific molecular substitution patterns. Given its simplicity and robust performance, this approach represents a significant progression in the development of crystalline organic semiconductors, and from which a next generation of crystalline **PDPP** materials may be efficiently designed and engineered.

Notes and references

1. M. Schwoerer and C. H. Wolf, *Organic Molecular Solids*, Wiley-VCH, 2007.
2. G. Schweicher, Y. Olivier, V. Lemaur and Y. H. Geerts, *Isr. J. Chem.*, 2014, **54**, 595-620.
3. H. Chung and Y. Diao, *J. Mat. Chem. C*, 2016, **4**, 3915-3933.
4. R. Li, W. Hu, Y. Liu and D. Zhu, *Acc. Chem. Res.*, 2010, **43**, 529-540.
5. M. E. Gershenson, V. Podzorov and A. F. Morpurgo, *Rev. Mod. Phys.*, 2006, **78**, 973-989.
6. E. D. Głowacki, H. Coskun, M. A. Blood-Forsythe, U. Monkowius, L. Leonat, M. Grzybowski, D. Gryko, M. S. White, A. Aspuru-Guzik and N. S. Sariciftci, *Org. Electron.*, 2014, **15**, 3521-3528.
7. M. Warzecha, J. Calvo-Castro, A. R. Kennedy, A. N. Macpherson, K. Shankland, N. Shankland, A. J. McLean and C. J. McHugh, *Chem. Commun.*, 2015, **51**, 1143-1146.
8. J. Calvo-Castro, M. Warzecha, I. D. H. Oswald, A. R. Kennedy, G. Morris, A. J. McLean and C. J. McHugh, *Cryst. Growth Des.*, 2016, **16**, 1531-1542.
9. J. Calvo-Castro, M. Warzecha, A. R. Kennedy, C. J. McHugh and A. J. McLean, *Cryst. Growth Des.*, 2014, **14**, 4849-4858.
10. J. Calvo-Castro, G. Morris, A. R. Kennedy and C. J. McHugh, *Cryst. Growth Des.*, 2016, **16**, 2371-2384.
11. J. Calvo-Castro, G. Morris, A. R. Kennedy and C. J. McHugh, *Cryst. Growth Des.*, 2016, **16**, 5385-5393.
12. O. Wallquist and R. Lenz, *Macromol. Symp.*, 2002, **187**, 617-629.
13. M. Grzybowski and D. T. Gryko, *Adv. Opt. Mater.*, 2015, **3**, 280-320.
14. D. Chandran and K.-S. Lee, *Macromol. Res.*, 2013, **21**, 272-283.
15. Y. Li, P. Sonar, L. Murphy and W. Hong, *Energy Environ Sci.*, 2013, **6**, 1684-1710.
16. J. Calvo-Castro, S. Maczka, C. Thomson, G. Morris, A. R. Kennedy and C. J. McHugh, *CrystEngComm*, 2016, **18**, 9382-9390.
17. N. A. Minder, S. Ono, Z. Chen, A. Facchetti and A. F. Morpurgo, *Adv. Mater.*, 2012, **24**, 503-508.
18. Y. Zhao and D. G. Truhlar, *Theor. Chem. Acc.*, 2008, **120**, 215-241.
19. J. Vura-Weis, M. A. Ratner and M. R. Wasielewski, *J. Am. Chem. Soc.*, 2010, **132**, 1738-+.
20. Y. Shao, L. F. Molnar, Y. Jung, J. Kussmann, C. Ochsenfeld, S. T. Brown, A. T. B. Gilbert, L. V. Slipchenko, S. V. Levchenko, D. P. O'Neill, R. A. DiStasio, Jr., R. C. Lochan, T. Wang, G. J. O. Beran, N. A. Besley, J. M. Herbert, C. Y. Lin, T. Van Voorhis, S. H. Chien, A. Sodt, R. P. Steele, V. A. Rassolov, P. E. Maslen, P. P. Korambath, R. D. Adamson, B. Austin, J. Baker, E. F. C. Byrd, H. Dachsel, R. J. Doerksen, A. Dreuw, B. D. Dunietz, A. D. Dutoi, T. R. Furlani, S. R. Gwaltney, A. Heyden, S. Hirata, C.-P. Hsu, G. Kedziora, R. Z. Khalliulin, P. Klunzinger, A. M. Lee, M. S. Lee, W. Liang, I. Lotan, N. Nair, B. Peters, E. I. Proynov, P. A. Pieniazek, Y. M. Rhee, J. Ritchie, E. Rosta, C. D. Sherrill, A. C. Simmonett, J. E. Subotnik, H. L. Woodcock, III, W. Zhang, A. T. Bell, A. K. Chakraborty, D. M. Chipman, F. J. Keil, A. Warshel, W. J. Hehre, H. F. Schaefer, III, J. Kong, A. I. Krylov, P. M. W. Gill and M. Head-Gordon, *Phys. Chem. Chem. Phys.*, 2006, **8**, 3172-3191.
21. J.-D. Chai and M. Head-Gordon, *Phys. Chem. Chem. Phys.*, 2008, **10**, 6615-6620.
22. S. F. Boys and F. Bernardi, *Mol. Phys.*, 2002, **100**, 65-73.
23. J. L. Bredas, D. Beljonne, V. Coropceanu and J. Cornil, *Chem. Rev.*, 2004, **104**, 4971-5003.
24. V. Coropceanu, J. Cornil, D. A. da Silva Filho, Y. Olivier, R. Silbey and J.-L. Bredas, *Chem. Rev.*, 2007, **107**, 926-952.
25. J. L. Bredas, J. P. Calbert, D. A. da Silva and J. Cornil, *Proc. Natl. Acad. Sci.U.S.A*, 2002, **99**, 5804-5809.
26. O. Ostroverkhova, *Chem. Rev.*, 2016, **116**, 13279-13412.
27. E. J. MacLean, M. Tremayne, B. M. Kariuki, J. R. A. Cameron, M. A. Roberts and K. D. M. Harris, *Cryst. Growth Des.*, 2009, **9**, 853-857.
28. B. Jiang, C. C. Du, M. J. Li, K. Gao, L. Kou, M. Chen, F. Liu, T. P. Russell and H. Wang, *Polym. Chem.*, 2016, **7**, 3311-3324.
29. J. Dhar, D. P. Karothu and S. Patil, *Chem. Commun.*, 2015, **51**, 97-100.
30. C. Kim, J. Liu, J. Lin, A. B. Tamayo, B. Walker, G. Wu and N. Thuc-Quyen, *Chem. Mater.*, 2012, **24**, 1699-1709.
31. T. Yamagata, J. Kuwabara and T. Kanbara, *Eur. J. Org. Chem.*, 2012, **2012**, 5282-5290.
32. T. Yamagata, J. Kuwabara and T. Kanbara, *Tetrahedron Lett.*, 2010, **51**, 1596-1599.

33. J. Mizuguchi, *Acta Crystallogr. Sect. Sect. E*, 2003, **59**, o472-o473.
34. R. L. Riggs, C. J. H. Morton, A. M. Z. Slawin, D. M. Smith, N. J. Westwood, W. S. D. Austen and K. E. Stuart, *Tetrahedron*, 2005, **61**, 11230-11243.
35. H. Akinori, T. Yoshiyuki, T. Yoshinori and M. Kazuo, *Chem. Lett.*, 2016, **45**, 211-213.
36. D. Hablot, P. Retailleau and R. Ziessel, *Chem. Eur. J.*, 2010, **16**, 13346-13351.
37. Y. Imura, T. Senju and J. Mizuguchi, *Acta Crystallogr. Sect. Sect. E*, 2005, **61**, o816-o818.
38. R. Sevincek, S. Celik, M. Aygun, S. Alp and S. Isik, *Acta Crystallogr. Sect. Sect. E*, 2010, **66**, o1546.
39. A. Iqbal, M. Jost, R. Kirchmayr, J. Pfenninger, A. Rochat and O. Wallquist, *Bull. Soc. Chim. Belg.*, 1988, **97**, 615-643.
40. H. Langhals, T. Potrawa, H. Noth and G. Linti, *Ang. Chem. Int. Ed. Engl.*, 1989, **28**, 478-480.
41. J. Mizuguchi, A. Grubenmann and G. Rihs, *Acta Crystallogr. Sect. B*, 1993, **49**, 1056-1060.
42. J. Mizuguchi and A. Arai, *Acta Crystallogr. Sect. Sect. E*, 2006, **62**, o4382-o4384.
43. J. Mizuguchi and S. Matsumoto, *Z. Kristallogr. - New Cryst. Struct.*, 2000, **215**, 195-196.
44. J. Kuwabara, T. Yamagata and T. Kanbara, *Tetrahedron*, 2010, **66**, 3736-3741.
45. D. Ostermann, R. Gompper and K. Polborn, *Private Communication*, 2005.